

# **GEOSYNTHETIC-REINFORCED EMBANKMENTS ON SOFT SOILS: NUMERICAL ANALYSIS OF THE STRAIN MOBILIZATION IN THE REINFORCEMENT DURING CONSOLIDATION PROCESS**

E.F. Ruiz, HUESKER Group, Bogotá D.C, Colombia

P.S. Hemsí, Faculty of Civil Engineering, Department of Geotechnics, Aeronautical Institute of Technology (ITA), São José dos Campos, Brazil

D.M. Vidal, Faculty of Civil Engineering, Department of Geotechnics, Aeronautical Institute of Technology (ITA), São José dos Campos, Brazil

## **ABSTRACT**

In this paper the behavior of geosynthetic-reinforced embankments constructed on soft cohesive foundations under undrained and partially drained conditions is examined by conducting a rigorous numerical analysis using the finite element method for a particular case study (a hypothetical road embankment). Special attention is given to the mobilized strains in the geosynthetic reinforcement at short and long-term working conditions considering the influence of the time-dependency of the system in terms of construction rate and excess pore pressure dissipation. The effects of reinforcement stiffness are also investigated.

The obtained numerical results illustrated the significant influence of consolidation process on the embankment performance (particularly in terms of mobilized reinforcement strains). A simple normalization procedure was carried out for the case study as an attempt to develop an analytical approach capable to predict the maximum mobilized reinforcement strain after a certain degree of consolidation in the soft soil foundation.

## **1. INTRODUCTION**

The use of geosynthetics as basal reinforcement in embankments constructed over soft soils provides technical and economic benefits by improving the stability of the structure, reducing horizontal displacements, homogenizing differential settlements, and reducing time of construction. An adequate design should include, however, more than routine limit equilibrium analyses, and should focus on understanding the soil-reinforcement interaction and mobilization of reinforcement strains during construction and with time, aspects that can be assessed with the use of finite elements simulations.

As reported by Bassett & Yeo (1988); Litwinowicz et al. (1994), Rowe et al. (1995), consolidation process in reinforced embankments may tend to increase strains in the reinforcement. Additionally, the foundation soil becomes stiffer as a result of the increase in undrained shear strength occurred due to consolidation, a fact that 'intuitively' may affect the mobilized tensile force in the reinforcement with time.

Accordingly, the main objective of this paper is to explore the influence of various factors including rate of construction, consolidation process and reinforcement stiffness on the mobilized short and long-term reinforcement strains observed in a typical road geosynthetic-reinforced embankment hypothetical case numerically analyzed via finite elements method.

A simplified methodology to ensure adequate end-of-construction stability (undrained stability) by estimating the required degree of reinforcement (minimum reinforcement stiffness modulus) was used in order to select an appropriate stiffness modulus for modeling the long term working conditions of the system. Considering adequate working conditions design parameters, instantaneous construction of the embankment was simulated as well as different construction rates. In addition, the dissipation of excess pore-water pressures with time was also properly modeled, evaluating the different effects on reinforcement strains. The influence of different reinforcement stiffness in the development of strains and horizontal displacements is also examined.

## 2. FINITE ELEMENT MODELING

### 2.1 Embankment geometry, mesh discretization and initial conditions

Figure 1 shows the geometry adopted for the study case representing a typical road embankment fill with design height,  $h = 2.30$  m and side slopes  $2H:1V$ , constructed over a soft clay foundation of 8.0 m depth, with undrained shear strength at the surface,  $S_{u0}$ , and a rate of increase of undrained shear strength with depth,  $\rho_c$ .

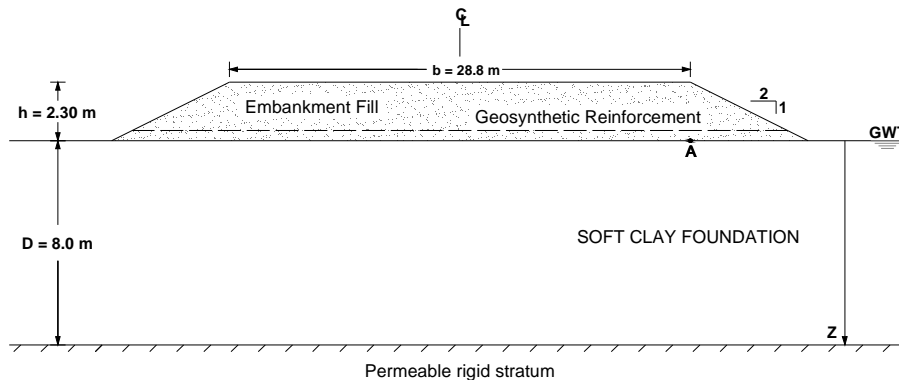


Figure 1. Considered embankment geometry and foundation soil stratigraphy.

The version 8.6 of the finite element program *PLAXIS* (Brinkgreve & Vermeer, 2004) was used in this study to simulate the embankment construction considering a small deformation and plane-strain analysis for the embankment cross-section. A typical “unstructured” element mesh with fifteen-node triangle elements with fine global coarseness was selected to discretize the fill and foundation soil. Five-node bar elements with elastic normal (axial) stiffness ( $EA$  or  $J$ ) were used to model the geosynthetic reinforcements. The considered position for the geosynthetic reinforcement was 0.40 cm above the fill/soft soil transition. The interface fill/reinforcement was assumed to follow an elastic perfectly-plastic model (Mohr-Coulomb criteria), and the interface parameter  $R_{inter}$  was chosen as being equal to 1.0, meaning that the interface soil/reinforcement was assumed to exhibit the same shear strength as the soils

immediately surrounding the interface. Initial geostatic state of stresses was numerically calculated by adopting the  $K^0$  procedure. Since phreatic level was defined at ground surface, the hydrostatic initial pore-water pressures were assessed automatically by defining this position.

## 2.2 Type of analyses

Two different numerical analyses were carried out in order to evaluate both undrained and partially drained behavior of the reinforced embankment. Firstly, a set of total stresses analyses (undrained) were carried in order to assess the required degree of reinforcement (minimum reinforcement stiffness modulus,  $J_{min}$ ) necessary to prevent short-term embankment failure as described by Hinchberger & Rowe, 2003. These analyses were conducted considering adequate partial factors ( $f_c = 1.3$ ,  $f_\phi = 1.2$  and  $f_\gamma = 1.1$ ) aiming to reproduce two combined Ultimate Limit States – ULS (i.e. maximum net embankment height and tensile failure of the reinforcement) as suggested by Hinchberger & Rowe (2003) and Rowe & Taechakumthorn (2011). The second group of analyses consisted in the simulation of the short and long term performance of the structure under working conditions (SLS) taking consolidation process into account (excess pore pressures development and dissipation). Therefore, all the applicable partial factors were considered equal to unity in this case ( $f_c, f_\phi$  e  $f_\gamma = 1.0$ ).

### 2.2.1 Total stresses analyses

The rapid undrained embankment construction was simulated by gradually turning on the gravity of consecutive embankment layers in automatically defined thick lifts at a rate corresponding to an instantaneous embankment construction scheme (construction time is neglected). The mechanical behavior of the foundation soft soil was modeled by using the Mohr-Coulomb constitutive model. Hence, it was assumed a soil with linear-elastic perfectly plastic stress-strain behavior, with fixed yield surface and non-associated plasticity rule. The foundation soil was assumed to undergo undrained loading (undrained analysis in terms of total stresses), disregarding the development of excess pore-water pressures in the soft soil. Consequently, it was necessary to consider a set of undrained soil parameters for the soft soil, as presented in the first part of Table 1. This set of parameters was selected based on typical values stated in the literature for Baixada Santista's hollocenic alluvial SFL ("*sedimentos fluvio-lagunares*") normally to slightly over-consolidated soft clays (Massad, 2009) and others properties reported in similar studies (e.g. Marinho, 2002; Hinchberger & Rowe, 2003).

### 2.2.2 Effective-stress analyses

It was adopted the identical modeling configuration previously considered in the total stresses undrained analyses (mesh type, global coarseness, boundary conditions, initial conditions, etc.). However, in this case the construction of the system was also simulated considering partially drained behavior of the soft soil, taking into account the effects of time in terms of construction rate, i.e., allowing partial dissipation of excess pore-water pressures during embankment construction. In addition, the 'primary' consolidation process taking place after the end of construction was also modeled ('primary' refers to no consideration of soil viscous behavior), allowing to study the short as well as long term response of the system. For this purpose, it was used the coupled Biot's consolidation model (Biot, 1941) which is the default consolidation model available in the software *PLAXIS*.

In order to simulate these features in terms of effective stresses, it was necessary to adopt adequate drained stiffness parameters for the foundation soil (i.e., drained Young's modulus,  $E'_{50}$ , and Drained Poisson's ratio,  $\nu$ ) as well as hydraulic conductivity for all materials involved based on values and relations reported in the literature (Brinkgreve & Vermeer, 2004; Rowe & Taechakumthorn, 2008; Massad, 2009). Table 2 shows the additional assumed parameters for both soft soil and embankment fill. The remaining geotechnical parameters required for the simulations corresponded to the same set of material properties described in Table 1.

Table 1. Geotechnical parameters considered for soft clay and sand fill for total stresses analysis.

Foundation soil	
Undrained shear strength at surface ( $S_{u0}$ )	5.0 kPa
Rate of increase in undrained strength with depth, ( $\rho_c$ )	1.50 kPa/m
Total friction angle ( $\phi$ )	0°
Saturated unit weight ( $\gamma_{sat}$ )	15 kN/m <sup>3</sup>
Undrained Poisson's ratio ( $\nu_u$ )	0.48
Undrained Young's modulus ( $E_u$ )	$E_u/S_u = 125$
Coefficient of lateral earth pressure at rest ( $K_0$ )	0.65
Embankment Fill	
Effective internal angle of friction ( $\phi$ )	37°
Effective cohesion intercept ( $c$ )	1.0 kPa
Compacted unit weight ( $\gamma_{bulk}$ )	20 kN/m <sup>3</sup>
Poisson's ratio for unloading-reloading ( $\nu_{ur}$ )	0.20
Secant triaxial stiffness modulus ( $E_{50}$ )	25000 kPa
Unloading-reloading stiffness modulus ( $E_{ur}$ )	75000 kPa
Oedometric stiffness modulus ( $E_{oed}$ )	25000 kPa
Power for stress-level dependency of stiffness ( $m$ )	0.50

Table 2. Geotechnical parameters considered for effective-stress analysis.

Foundation soft soil	
Drained Poisson's ratio ( $\nu$ )	0.33
Drained Young's modulus ( $E'_{50}$ )	$E'_{50} = (2(1 + \nu)E_u) / 3$
Vertical hydraulic conductivity ( $k_v$ )	$1 \times 10^{-4}$ m/day
Horizontal hydraulic conductivity ( $k_h$ )	$k_h/k_v = 3$
Embankment Fill and Stiff stratum	
Horizontal and vertical hydraulic conductivity ( $k_h, k_v$ )	1.0 m/day

### 3. RESULTS AND DISCUSSIONS

#### 3.1 Determination of the minimum secant reinforcement stiffness modulus

Based on the methodology proposed by Hinchberger & Rowe (2003), total stresses numerical analyses results allowed to estimate a value of 3.44% for the allowable compatible reinforcement strain ( $\epsilon_a$ ). Further details about this estimation can be founded in Ruiz (2013) and Ruiz et al. (2013).

By carrying out a conventional limit equilibrium analysis (rotational slip circle, modified Bishop method), the required reinforcement force ( $T_{ro}$ ) to ensure stability (i.e. safety factor of 1.0 for factored soils properties for ULS) after the instantaneous construction of fill thickness of 2.30 m was evaluated as being equal to 50 kN/m. In this manner, the assessment of the minimum required reinforcement stiffness ( $J_{min}$ ) can be realized as follows:  $J_{min} = \alpha_r T_{ro} / \epsilon_a = 1.15 \times 50 \text{ kN/m} / 0.0344 = 1672 \text{ kN/m}$  (where  $\alpha_r$  was considered equal to 1.15 according to Ruiz (2013)).

#### 3.2 Mobilized reinforcement strains at the end of construction, $\epsilon_{ro}$

Assuming an instantaneous construction procedure and by considering the minimum required reinforcement tensile stiffness modulus ( $J_{min} = 1672 \text{ kN/m}$ ) previously calculated as input value for the reinforcement as well as the parameters defined for working condition representation, it was possible to obtain from finite elements simulations a maximum mobilized strain in the reinforcement ( $\epsilon_{ro}$ ) of 0.95 % and a maximum mobilized reinforcement tensile force ( $T_{mob,o}$ ) of 15.93 kN/m at the end of construction as a result of the placement of the embankment fill at the required design height ( $h = 2.30 \text{ m}$ ). This maximum mobilized reinforcement strain at the end of construction ( $\epsilon_{ro}$ ) can be also calculated in an approximate approach by carrying out a limit equilibrium analysis and evaluating the force in the reinforcement ( $T_{ro,sls}$ ) required to achieve a safety factor of 1.0 considering factored soils properties for SLS conditions. For this case study, it was obtained a force ( $T_{ro,sls}$ ) of 14.50 kN/m from the limit equilibrium analysis described before. By considering this value in combination with  $J_{min}$ , it was possible to asses an approximated maximum mobilized reinforcement strain at the end of construction ( $\epsilon_{ro,ap}$ ) equal to 0.86 %, which is a similar result in comparison with the obtained from the numerical simulation (0.95%).

#### 3.3 Effect of the embankment construction rate (partially drained behavior)

The examination of the effects of the construction rate and the corresponding partial consolidation during embankment construction on the mobilized reinforcement strains are briefly presented in Table 3 for three different construction rates. For these simulations, the reinforcement  $J$  was assumed equal to  $J_{min} = 1672 \text{ kN/m}$ . As expected, the most prolonged period of construction (0.25 m per week) produced the mobilized reinforcement strain at the end of construction to be slightly higher compared to the other cases.

Table 3. Mobilized reinforcement strains at the end of construction.

Construction rate	$\epsilon_{ro}$
Instantaneous construction	0.95 %
1 m / week	0.98 %
0.25 m / week	1.01 %

### 3.4 Effect of the primary consolidation process (long-term behavior)

With the purpose of estimating the evolution of mobilized reinforcement strains along time, the consolidation process was numerically simulated considering 14 years of service life after the end of construction of the embankment properly reinforced, i.e., with  $J = J_{min}$ .

Figure 2 shows the evolution of mobilized reinforcement strains during soil consolidation. As can be noticed, after about 14 years (degree of consolidation,  $U \approx 90\%$ ) of dissipation of the excess water pore-pressures, the mobilized reinforcement strain increased to 1.46 % due to consolidation, from the value of 0.95 % at the end of construction.

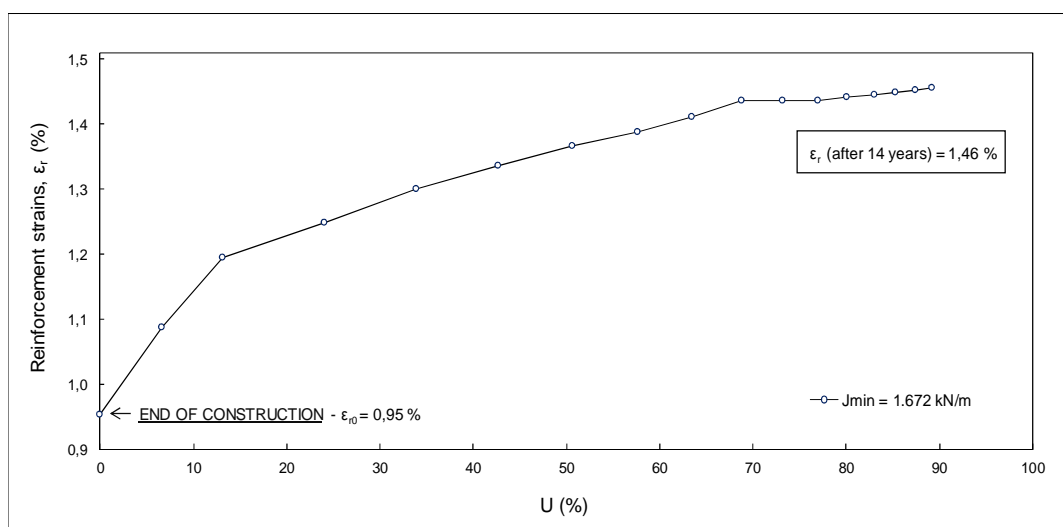


Figure 2. Mobilized reinforcement strains along the dissipation of the excess of pore-water pressures.

The results illustrate the fact that the effect of mobilization of additional strains as a result of consolidation of the soft soil is more important during the beginning of consolidation after the end of construction (period with higher potential degree of dissipation). Therefore, prior to the conclusion of consolidation process, the reinforcement strains tend to remain constants (disregarding other aspects as creep in both reinforcement and/or soil among others).

### 3.5 Influence of the reinforcement stiffness

The performance of a reinforced embankment in terms of serviceability conditions (e.g., deformations, displacements, etc.) can be enhanced by selecting a reinforcement with stiffness modulus greater than the minimum required to guarantee undrained stability ( $J_{min}$ ). In this manner, the behavior of the system was simulated considering reinforcements with stiffness moduli two and three times higher than the minimum required  $J_{min}$  (i.e.  $2 \times J_{min}$  and  $3 \times J_{min}$ ).

Figures 3 and 4 show the influence of reinforcement stiffness on mobilized reinforcement strains at end of construction and along primary consolidation (total and relative values correspondingly). As can be pointed out from

the results, the adoption of a stiffer geosynthetic reinforcement leads to a reduction in both short and long-term mobilized reinforcement strains, not only in magnitudes, but also in the percentage of increase over time. This percentage of increase in mobilized strain for the stiffest reinforcement ( $3 \times J_{min}$ ) was of only 28 % in about 14 years.

The results in Figure 4 show that the ratio  $\epsilon_r / \epsilon_{r0}$  at any time after construction depends on the reinforcement stiffness modulus. Therefore, an attempt to normalize the evolution of  $\epsilon_r$  with time requires the consideration of  $J$ . Also, it is observed that the ratio  $\epsilon_r / \epsilon_{r0}$  does not increase linearly with increasing  $J$ .

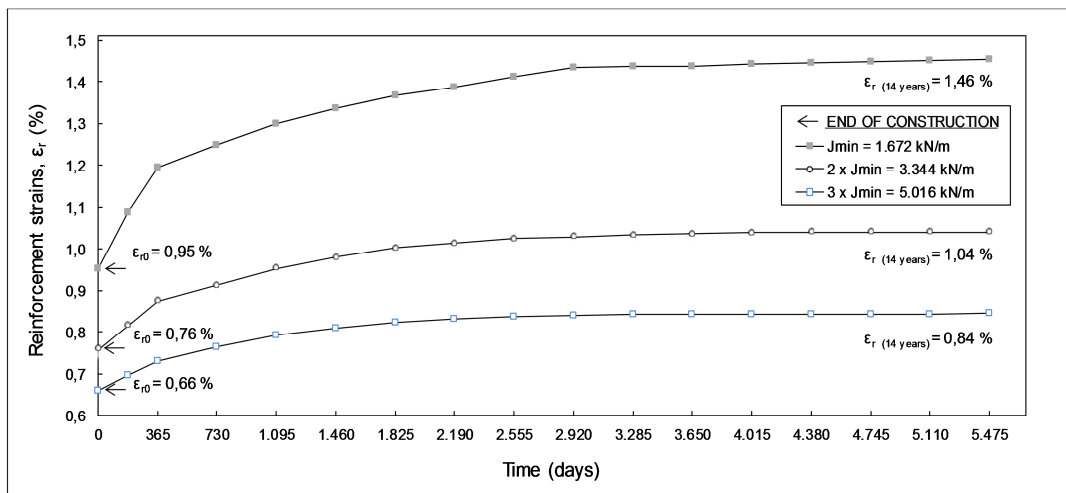


Figure 3. Influence of reinforcement stiffness on mobilized reinforcement strains along the consolidation

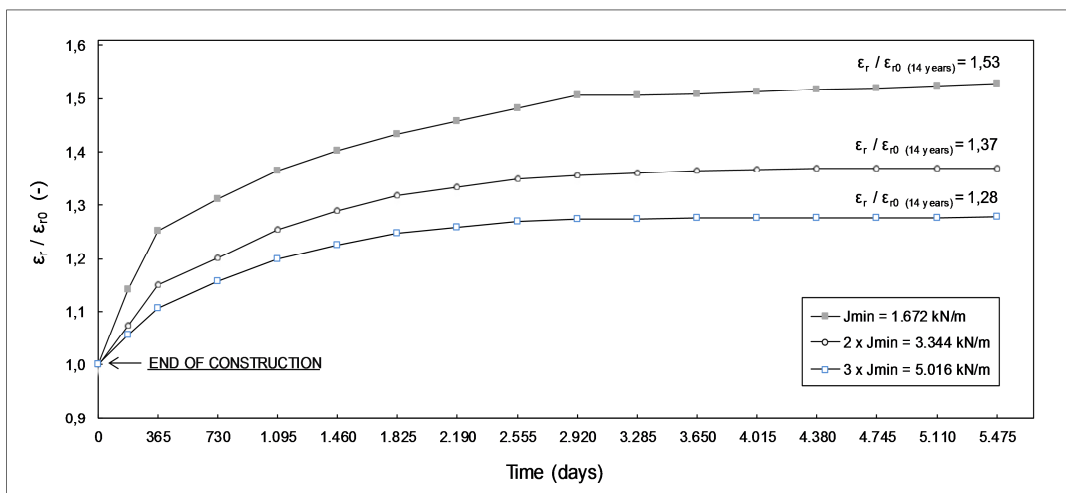


Figure 4. Influence of reinforcement stiffness on relative evolution of mobilized reinforcement strains with time.

In order to establish a normalized relation to assess an approximated value for the mobilized strain in the reinforcement at any time after the embankment construction ( $\varepsilon_r$ ) for different values of  $J$  other than the ones simulated (Figure 4), the following normalization relation was developed for  $\varepsilon_r$  as a function of  $\varepsilon_{r0}$ , with a non-linear dependence on  $J$ :

$$\frac{\varepsilon_r - \varepsilon_{r0}}{\varepsilon_{r0}} \sqrt{\frac{J_{min}}{J}} \quad [1]$$

$J$  is the specific reinforcement tensile modulus ( $\geq J_{min}$ ) and  $\varepsilon_{r0}$  is the maximum mobilized reinforcement stiffness at the end of construction, which can be approximately estimated by a simplified procedure (e.g. limit equilibrium as described in section 3.2). Time is expressed in terms of the dimensionless parameter referred as maximum degree of consolidation ( $U$ ). The results of the normalization of both the  $x$  and  $y$  axis are presented in Figure 5.

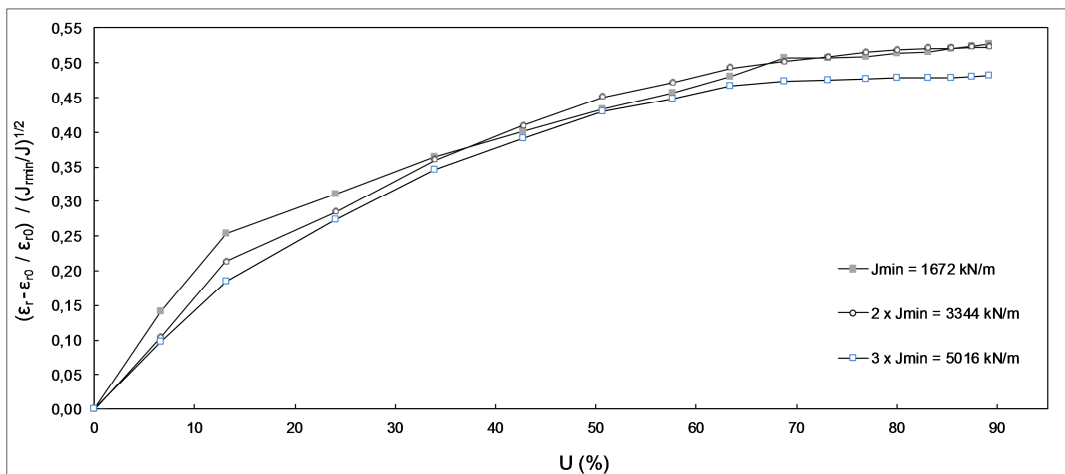


Figure 5. Normalization chart (reinforcement stiffness/strains/ $U$ ).

It is worth to remark that this normalized chart was developed for academic intents, and its estimations are only valid for the case study considered herein (embankment geometry, soils stratigraphy, geotechnical parameters, etc.).

Furthermore, the horizontal displacements in the soft soil layer underneath the toe of the embankment that were numerically calculated for the cases analyzed are shown in Figure 6 as the displacement profiles along soil depth. As illustrated in Figure 6, an important effect of reinforcement stiffness is to reduce not only short-term but also of long-term horizontal displacements. As an example, the adoption of a reinforcement three times stiffer than the minimum required for short term stability led to a reduction of ~ 4 cm in lateral displacement for this case study.

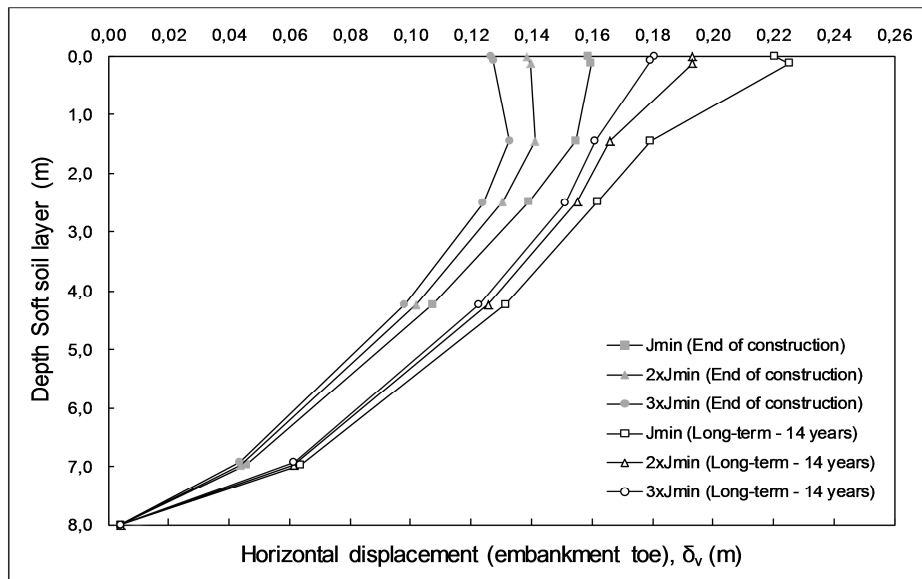


Figure 6. Variation of horizontal displacements with reinforcement stiffness (end of construction and long-term).

#### 4. CONCLUSIONS

This article studied the mobilization of reinforcement strains in geosynthetic-reinforced embankments constructed over soft soil foundation at working conditions. A comprehensive series of finite element analyses were conducted in order to simulate the embankment behavior for a hypothetical case. In this manner, the short and long-term response of the system was examined considering various factors such as the compatible allowable reinforcement strain, tensile stiffness of the reinforcement, construction rate and consolidation process of the foundation soil. The following conclusions can be drawn from the studies presented in this article:

- Under working conditions, consolidation process after the end of embankment construction induces additional strains in the reinforcement. This maximum observed increase in mobilized reinforcement strain was about 53 % for the case of  $J_{min}$ .
- As expected, a slower construction rate provokes slightly higher mobilized reinforcement strains as a consequence of partial consolidation occurred during construction.
- The maximum mobilized reinforcement strain at the end of construction obtained from Hinchberger & Rowe (2003) methodology combined with limit equilibrium analysis showed consistency in comparison with the numerical result, which represents a preliminary validation of this approximated approach.
- A normalization chart was developed as an initial approximated methodology to study additional mobilization of strains in the reinforcement as a result of consolidation process (disregarding soil and reinforcement creep).

- The short and long-term performance of the embankment in terms of mobilized reinforcement strains can be improved by increasing the reinforcement stiffness. The short and long-term lateral displacements were also substantially reduced by the use of higher values of reinforcement tensile stiffness.

## REFERENCES

Bassett, R. H. & Yeo, K. C. (1988). The behaviour of a reinforced trial embankment on soft shallow foundations. *International Geotechnical Symposium on Theory and Practice of Earth Reinforcement*, Fukuoka, pp. 371–376.

Biot, M. A. (1941). General theory of three-dimensional consolidation. *Journal of Applied Physics*, 12, 155–164.

Brinkgreve, R.B.J. and Vermeer, P.A. (2004). *Material models manual - Plaxis finite element code for soil and rock analysis-Version 8.6*, Balkema, Rotterdam, The Netherlands.

Hinchberger, S.D. and Rowe, R. K. (2003). Geosynthetic reinforced embankments on soft clay foundations: predicting reinforcement strains at failure. *International Journal of Geotextiles and Geomembranes*, No.21, USA.

Litwinowicz, A., Wijeyakulasuriya, C. V. and Brandon, A. N. (1994). Performance of a reinforced embankment on a sensitive soft clay foundation. *Proceedings 5th International Conference on Geotextiles, Geomembranes and Related Products*, Singapore.

Marinho de Moraes, C. (2002). Aterros reforçados sobre solos moles – Análise numérica e analítica. *Master's dissertation*, UFRJ, Rio de Janeiro, Brazil.

Massad, F. (2009). *Solos marinhos da baixada santista - características e propriedades geotécnicas*. 1. Ed. Oficina de textos, 2009. V. 1. 247p, São Paulo, Brazil.

Rowe, R. K., Gnanendran, C. T., Landva, A. O. & Valsangkar, A. J. (1995). Construction and performance of a full-scale geotextile reinforced test embankment, Sackville, New Brunswick. *Canadian Geotechnical Journal*, 32, No. 3, 512–534, Canada.

Rowe, R.K. and Taechakumthorn, C. (2008). Combined effect of PVDs and reinforcement on embankments over rate-sensitive soils. *Geotextiles and Geomembranes*, Vol. 26(3), pp. 239-249.

Rowe, R.K and Taechakumthorn, C. (2011). The interaction between reinforcement and vertical drains and effect of performance of embankments on soft ground. *Soil and Rocks*, 34(4): 261-275, São Paulo, Brazil.

Ruiz, E.F. (2013). Geosynthetic-reinforced embankments on soft soils: numerical analysis of the strain mobilization in the reinforcement at failure, service condition and staged construction. *Master thesis*. Aeronautics Institute of Technology, São José dos Campos, Brazil.

Ruiz, E.F., Hemsí, P.H. and Vidal, D.M. (2013). Numerical analysis of reinforcement strains at failure for reinforced embankments over soft soils. *Soil and Rocks*, 36(3): 299-307, São Paulo, Brazil.